A GAP-VARYING ELECTROSTATIC TRANSDUCER UTILIZING FERROFLUID-BASED ACTUATION FOR MOTION HARVESTING

T. Galchev, D. Barutçu, and O. Paul
Department of Microsystems Engineering (IMTEK), University of Freiburg, Germany

ABSTRACT

This paper provides the electrical characterization of the gap-varying ferrofluid-based electrostatic springless proximity inertial harvester (SPIH). The SPIH is a multi-axis motion harvesting structure capable of three-dimensional low-frequency operation from human or environmental application scenarios among others. The device structure consists of an array of electrostatic transducers that are interconnected and filled with a magnetic fluid. A spherical magnet serves as the proof mass. Mechanical energy is transferred to each transducer magnetically. A hydrostatic pressure in the magnetic fluid actuates the top plate of each variable capacitor. Each 2-mm-diameter transducer is capable of producing between 0.05-4.2 nJ of energy per actuation cycle at bias voltages of 10-100 V under controlled experiments. Harvesting multi-axial motion from random hand movements (including *x*- and *y*-axis translation and rotation) is demonstrated to produce peak power levels as high as 3 nW (with only one transducer from the array connected) and by using a 10 V initial bias.

INTRODUCTION

Energy harvesting power sources have been studied at length over the past decade as possible replacements and/or supplements to battery powered operation for wireless systems. Energy in the form of motion is among the most popular and important sources of renewable power. However, a great deal of the focus has been on harvesting linear vibrations from machinery, moving vehicles, and other man made sources. On the other hand, applications like body area networks (BAN) and environmental and structural health monitoring require a greater degree of harvester versatility with respect to bandwidth, input amplitude, and axis of motion. Multi-axis harvesters (MAH), important for human powered applications, have recently become a topic of increased investigation. Most can be grouped in two general categories including in-plane micromachined varieties [1-4] and devices that include a freely moving mass [5-8] that is not suspended to the casing.

A new MAH concept was recently presented [9] that uses a suspension-less spherical inertial mass to capture multi-axial human motion. The design features an array of transducer cells that can couple to the rolling magnetic proof mass, absorb mechanical energy, and convert it electrostatically. This arrangement has been shown to be less sensitive to the exact magnet position and orientation and thereby offers greater design flexibility and design versatility. The previously presented concept is further elaborated in this paper. Additionally, the electrostatic gap-varying transducer cells are electrically characterized and energy harvesting from simple hand movements is demonstrated.

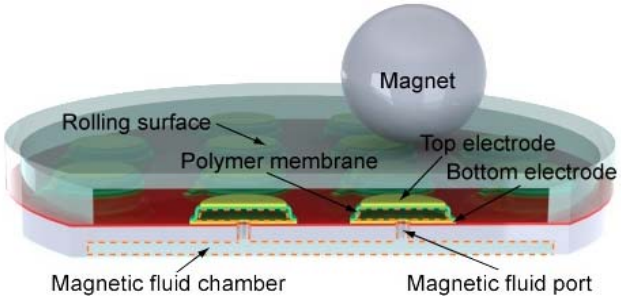

Figure 1. Illustration of the springless proximity inertial harvester (SPIH)

DEVICE STRUCTURE AND FABRICATION

An illustration of the springless proximity inertial harvester (SPIH) can be seen in Figure 1. It has a spherical magnetic proof mass that is free to roll. The proof mass captures kinetic energy, after which an array of electrostatic transducer cells converts it into electricity. The magnet never comes in contact with the transducer cells, which is important for long-term reliability. Instead energy is transferred via magnetic coupling. The link between the transducers and the magnet is established via a ferrofluid. These are colloidal liquids made of nanometer-size magnetic particles. This liquid becomes magnetized in the presence of a magnetic field and produces a hydrostatic pressure against the movable top electrode of the transducer cell thereby varying the capacitance.

Fabrication of the transducers (Figure 2) was previously discussed in detail [9] and consists of a three-wafer process. The transducers are surface micromachined and use a 10 μm sacrificial photoresist to release a Parylene membrane, about 4 μm in thickness, after which fluidic interconnects are made using DRIE. Electrodes are made from 50/500 nm Cr/Au. The most critical process step is the bonding of the bottom recessed Pyrex cap that forms the ferrofluid chamber. In order to prevent air bubbles from forming inside the device, a process to bond the cap while inside the ferrofluid solution was developed. A UV curable epoxy is used to seal the fluid reservoir. The ferrofluid chamber has a combined depth of 400-500 μm taking into account the combined recess in the silicon and Pyrex wafers. A photograph of an assembled SPIH with 2-mm-diameter transducers is shown in Figure 3.

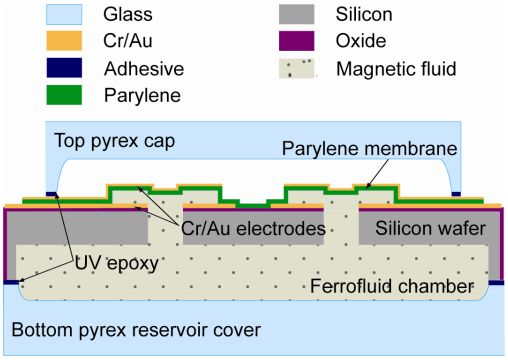

Figure 2. Process flow summary. The variable-gap transducers are surface micromachined on a silicon wafer and enclosed from both sides using Pyrex caps. ‘

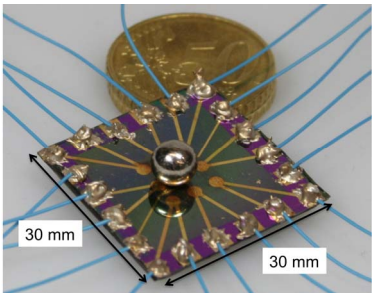

Figure 3. Photograph of the SPIH next to a 50 Euro cent coin.

FERROFLUID ACTUATION

The ferrofluid-based actuation process is illustrated in Figure 4. When a magnetic field is applied over the transducer cell a hydrostatic pressure, P_{mag}, is generated in the ferrofluid according to [10]

$$P_{mag} = \mu_o M_s \int_{H_b}^{H_t} dH, \qquad (1)$$

where μ_0 is the permeability, M_s is the saturation magnetization, and H_t and H_b refer to the magnitude of the magnetic field at the top and bottom of the fluid column respectively. The red (left) curve in Figure 5 shows the measured magnetic flux density generated by a cubic NdFeB magnet (5×5×5 mm^3) as a function of distance, *d,* from the top of the movable electrode. Measurements were made using a Bell 6010 Teslameter. In order to ease the calculation of hydrostatic pressure two simplifications are made: 1) The magnetic field is assumed to vary through the depth of the fluid column as a third-order polynomial function extracted from the measured data in Figure 5; 2) The magnetic field is assumed to be uniform across the plane of the wafer. The black (right) axis of Figure 5 is used to plot the hydrostatic pressure with respect to the fluid column height, *h*. The column height, or in other words, the depth of the magnetic fluid reservoir can be designed to be ≤1 mm in the present process. Therefore the expected hydrostatic pressure will be in the range of 4-6 kPa. A wealth of previous art exists that allows the designer to then convert this uniform pressure

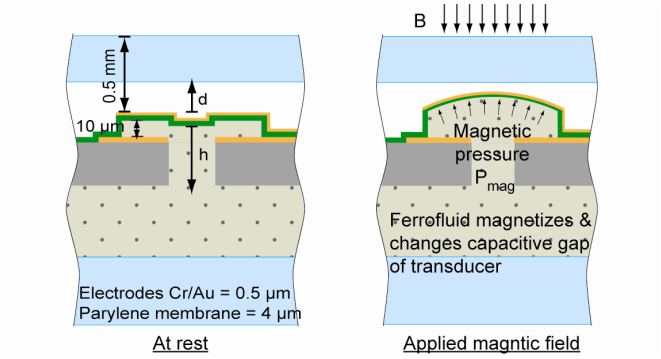

Figure 4. Schematic method of operation. An applied magnetic field magnetizes the ferrofluid and varies the capacitive gap in the transducer.

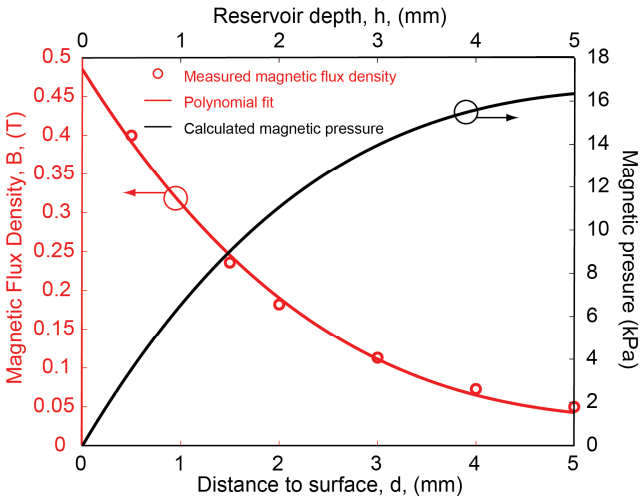

Figure 5. Red curve shows the measured magnetic flux density, B, as a function of distance from the surface of the transducer, while the black curve shows the simulated magnetic pressure as a function of ferrofluid reservoir depth at a fixed B.

applied on the thin membrane into a deflection, and subsequently into a capacitance change. Finally, the energy that can be generated per actuation cycle is given as

$$E_{cycle} = \frac{1}{2}\Delta C V^2, \qquad (2)$$

where V is the applied pre-bias voltage. Maximum capacitance change can be achieved through careful optimization of the Cr/Au layer thickness which defines the effective membrane stiffness, initial inter-electrode gap, and magnetic pressure.

TRANSDUCER CHARACTERIZATION

Harvested energy is experimentally measured. Sets of controlled experiments were performed where the SPIH was mounted on an automated *xyz*-stage while a cubic magnet (5×5×5 mm^3) was suspended above. A voltage-constrained cycle was carried out to measure the energy generation

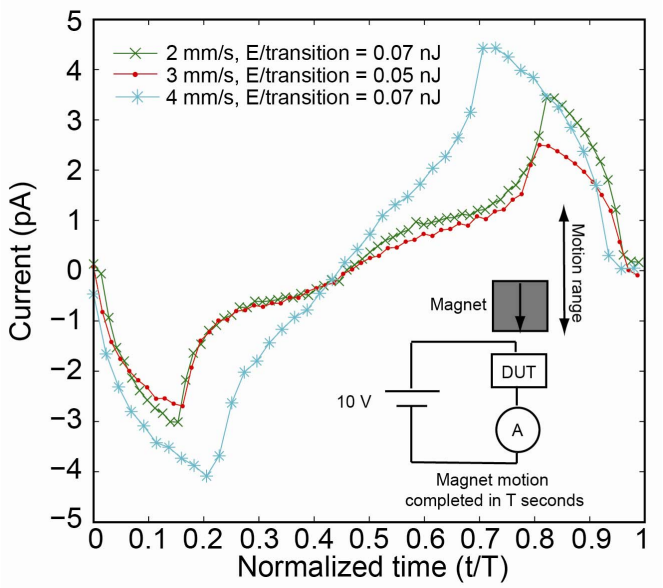

Figure 6. Current is measured while the magnet is translated perpendicular to the transducer surface (see inset) at different velocities. The capacitor transitions from ($C_{min} \rightarrow C_{max} \rightarrow C_{min}$).

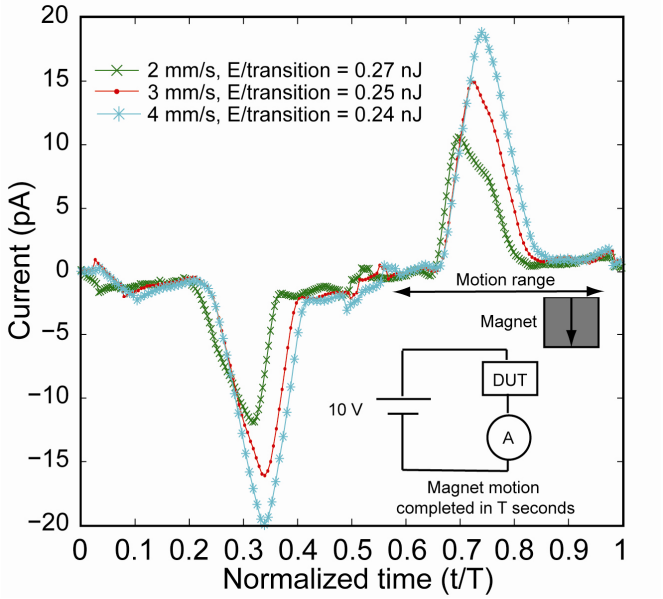

Figure 7. Current is measured while the magnet is scanned horizontally across the transducer surface (see inset) at different velocities. The capacitor transitions from ($C_{max} \rightarrow C_{min} \rightarrow C_{max}$).

capability. A Keithley 6487 picoammeter is used to measure current at a bias voltage of 10 V. Figure 6 shows the results of varying the capacitance by moving the magnet perpendicular to the transducer in the *z*-direction. The actuation cycle starts at the bottom where the membrane is deflected and consequently capacitance is minimum. One full cycle moves the magnet up and then back down again ($C_{min} \rightarrow C_{max} \rightarrow C_{min}$). This motion is repeated at different velocities. The bias voltage is kept fixed while the capacitance is varied. The plot is normalized so that currents generated at different speeds can be displayed on top of each other for comparison. Additionally one must note that since there is no diode to prevent current backflow there are two current spikes, one produced during energy generation and one produced during capacitor relaxation as charge is again brought back by the priming source. A comparable experiment is shown in Figure 7, however this time the motion of the magnet is parallel to the surface of the transducer. In this case the capacitance undergoes a slightly different cycle ($C_{max} \rightarrow C_{min} \rightarrow C_{max}$) since the magnet starts and ends away from the transducer. To compute harvested energy, half of the current (only the energy generation half) is integrated over one translation period and multiplied with the applied potential difference. Horizontal magnet motion is shown to produce a higher output energy, ≈0.25 nJ/transition, with magnet velocities of 2-4 mm/s, as compared with vertical magnet motion which generated ≈0.05 nJ/transition. In the case of horizontal motion, there is an observable reduction of energy with increasing magnet speed, which can be interpreted as being the result of damping in the dynamic response of the device. For vertical motion, harvested energy reduces significantly as compared with horizontal motion. The vertical motion experiments were performed mainly for

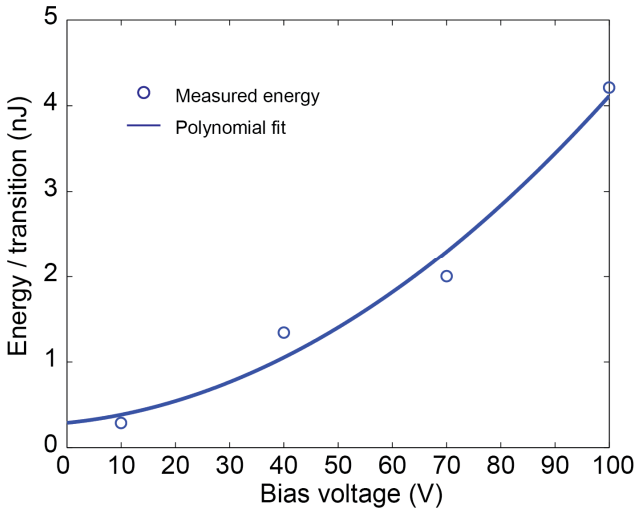

Figure 8. Energy produced per transition is measured as a function of bias voltage for the horizontal magnet translation. The velocity is 2 mm/s.

their academic value since the horizontal motion is more closely related to a spherical magnet rolling on the surface. The reduction in energy seen in the vertical translation may be from two possible sources. First, even when the magnet is at rest in the farthest position, there is still a non-zero external magnetic field resulting in a hydrostatic force at all times. Additionally, fluid motion is different in the two scenarios. In the case of horizontal translation the magnet can be thought of as dragging in the fluid and then helping to empty the thin and long capacitive-gap, whereas in the case of vertical motion the fluid may have a harder time moving out from within the electrodes resulting in lower capacitance

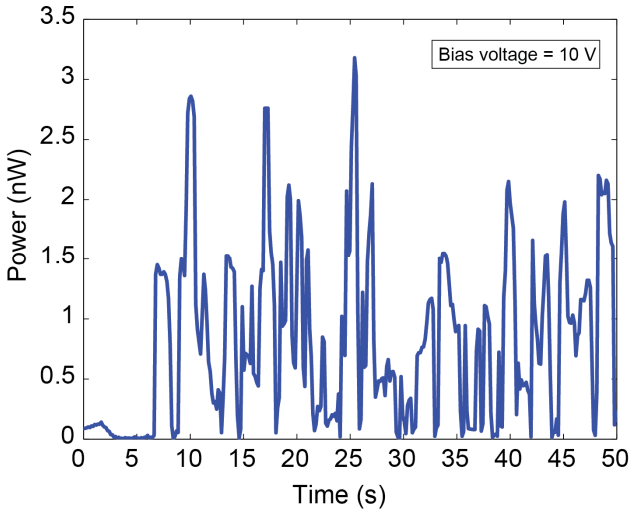

Figure 9. Power is measured while a 6 mm-diameter spherical magnet is placed on the SPIH and allowed to roll freely as the harvester is moved by hand.

change. Energy is plotted as a function of bias voltage in Figure 8. The measurements are made using horizontal translation at a velocity of 2 mm/s. There is a deviation from the square law relationship expected from (2). A higher increase in converted energy is expected. One possible explanation is that there is measurement error at higher bias voltages. There could be bias voltage instability or insufficient bandwidth to capture the larger current peaks. These issues have to be investigated further.

ENERGY HARVESTING TEST RESULTS

A preliminary experiment was performed to measure the energy producing capability of the SPIH under multi-axial motion. A 6-mm-diameter NdFeB spherical magnet was used. One transducer cell in the center of the SPIH was connected to the picoammeter in the same manner as the previous experiments. Current was measured continuously while the harvester was held in the operator's hand and subjected to lateral *x*- and *y*-axis translations as well as rotation around both axes in a random manner. While acceleration was not measured simultaneously, it is assumed to be quite low and well within the range expected from regular human motion. Tethering the SPIH to the sensitive current measurement equipment did not allow for large or rapid movements. The results of this experiment are shown in Figure 9, where a single transducer cell generated over 3 nW of instantaneous power.

CONCLUSION

This paper presented the electrical characterization of the gap-varying springless proximity inertial harvester. The multi-axis motion harvester uses a spherical magnetic proof mass to pass mechanical energy within a gap-varying electrostatic transducer by magnetizing an integrated magnetic fluid. In this manner the proof mass never comes in contact with the transducers. A prototype with an array of 2-mm-diameter transducers was shown to be capable of producing 0.05-4.2 nJ of energy per actuation cycle when biased in the range of 10-100 V. For the first time energy harvesting was demonstrated using the SPIH. Simple translational and rotational hand movements were able to generate power levels between 0.5-3 nW using only one connected transducer under a very weak bias of 10 V.

ACKNOWLEDGEMENTS

This work was supported by the Alexander von Humboldt Foundation.

REFERENCES

[1] U. Bartsch, J. Gaspar, and O. Paul, "A 2D electret-based resonant micro energy harvester," in *IEEE Int. Conf. on Microelectromechanical Systems (MEMS)*, USA, pp. 1043-6, 2009.

[2] U. Bartsch, J. Gaspar, and O. Paul, "Low-frequency two-dimensional resonators for vibrational micro energy harvesting," *J. of Micromech. and Microeng.,* vol. 20, p. 035016 (12 pp.), 2010.

[3] J. L. Fu, Y. Nakano, L. D. Sorenson, and F. Ayazi, "Multi-axis AlN-on-silicon vibration energy harvester with integrated frequency-upconverting transducers " in *IEEE Int. Conf. on Microelectromechanical Systems (MEMS)*, Paris, France, pp. 1269-1272, 2012.

[4] L. Huicong, S. Bo Woon, W. Nan, C. J. Tay, Q. Chenggen, and L. Chengkuo, "Feasibility study of a 3D vibration-driven electromagnetic MEMS energy harvester with multiple vibration modes," *J. of Micromech. and Microeng.,* vol. 22, p. 125020, 2012.

[5] M. E. Kiziroglou, C. He, and E. M. Yeatman, "Rolling rod electrostatic microgenerator," *IEEE Trans. on Industrial Electronics,* vol. 56, pp. 1101-8, 2009.

[6] P. Pillatsch, E. M. Yeatman, and A. S. Holmes, "A scalable piezoelectric impulse-excited generator for random low frequency excitation," in *IEEE Int. Conf. on Microelectromechanical Systems (MEMS)*, pp. 1205-8, 2012.

[7] B. J. Bowers and D. P. Arnold, "Spherical, rolling magnet generators for passive energy harvesting from human motion," *J. of Micromech. and Microeng.,* vol. 19, p. 094008 (7 pp.), 2009.

[8] T. Galchev, R. Raz, and O. Paul, "A new multi-dimensional low-frequency springless proximity inertial harvester for converting human and environmental motion," in *PowerMEMS,* Atlanta, USA, pp. 117-120, 2012.

[9] T. Galchev, R. Raz, and O. Paul, "An electrostatic springless inertial harvester for converting multi-dimensional low-frequency motion " in *IEEE Int. Conf. on Microelectromechanical Systems (MEMS)*, Taipei, Taiwan, pp. 102-105, 2013.

[10] R. E. Rosensweig, *Ferrohydrodynamics*. Cambridge University Press, 1985.